Schizophrenia Bulletin vol. 51 no. S2 pp. S149–S159, 2025
https://doi.org/10.1093/schbul/sbae160

SUPPLEMENT ARTICLE

Differential Association of Schizotypy Dimensions With Brain Structural Connectivity and Moderation by Schizophrenia Polygenic Risk

Jonas Hoffmann[1], Tina Meller[1,2], Carlo Maj[3], Per Hoffmann[4], Andreas J. Forstner[3,4,5], Markus M. Nöthen[4], and Igor Nenadić[1,2,6,*]

[1]Cognitive Neuropsychiatry Laboratory, Department of Psychiatry and Psychotherapy, Philipps-Universität Marburg, Marburg 35039, Germany; [2]Center for Mind, Brain, and Behavior (CMBB), Universities of Marburg, Gießen, and Darmstadt, Marburg 35032, Germany; [3]Center for Human Genetics, Philipps Universität Marburg 35033, Marburg, Germany; [4]Institute of Human Genetics, University of Bonn, School of Medicine & University Hospital Bonn, Bonn 53127, Germany; [5]Institute of Neuroscience and Medicine (INM-1), Research Center Jülich, Jülich 52428, Germany[6]LOEWE Center DYNAMIC, University of Marburg, 35032 Marburg, Germany

[*]To whom correspondence should be addressed; Department of Psychiatry and Psychotherapy, Philipps Universität Marburg, Rudolf-Bultmann-Str. 8, 35039 Marburg, Germany; tel: +49-6421-58-65002, fax: +49-6421-58-68939, e-mail: nenadic@staff.uni-marburg.de

***Objective*: Schizotypy as a psychosis proneness marker has facilitated the study of schizophrenia spectrum models, linking phenotypic psychosis risk to brain structural and functional variation. However, association studies to structural connectome markers are limited and often do not consider relations to genetic risk. We tested the hypothesis that dimensions of schizotypy (rather than overall phenotype risk burden) are related to fiber tract integrity and that this is moderated by polygenic schizophrenia risk (or resilience). *Design*: In a cohort of 346 psychiatrically healthy subjects, we obtained diffusion tensor imaging, schizotypy using O-LIFE (Oxford-Liverpool Inventory of Feelings and Experiences), and polygenic risk scores (PRS) for schizophrenia risk and resilience to schizophrenia. Using FSL and TBSS (tract-based spatial statistics), we first analyzed the association between O-LIFE and fractional anisotropy (FA) for the anterior thalamic radiation, uncinate fascicle, and cingulum bundle, as well as moderation analyses with PRS scores. *Results*: O-LIFE dimensions were differentially associated with structural connectivity, in particular, negative schizotypy positively to right uncinate FA, positive schizotypy negatively to right cingulum and disorganized schizotypy negatively to left cingulum. In disorganized schizotypy the association was moderated by schizophrenia PRS. *Conclusions*: Our results support a neurobiological continuum model of structural connectivity across psychosis proneness, emphasizing differential association with different schizotypy facets. Genetic schizophrenia risk, however, appears to impact only some of these associations, highlighting the need for further studies to understand the contribution of other genetic and/or environmental factors.**

Key words: diffusion tensor imaging (DTI)/Oxford-Liverpool inventory of feelings and expressions (O-LIFE)/schizotypy/tract-based spatial statistics (TBSS)

Introduction

Previous studies investigating the biological basis of the psychosis spectrum indicate an overlap between schizotypy and schizophrenia across multiple environmental, neurocognitive, neurobiological, and behavioral domains[1] suggesting gradual changes along the spectrum.[2] Thus, examining the neurobiology of schizotypy might help gain further understanding of the etiology and development of schizophrenia spectrum disorders.[3]

Schizotypy can be defined as a set of personality traits divided into 3 distinct dimensions, which can be measured psychometrically across the general population using self-report questionnaires.[4] This multidimensional structure includes positive schizotypy (characterized by delusions, suspiciousness, magical thinking, as well as hallucinations[5]), negative schizotypy (containing aspects like social anhedonia and diminished emotional experience and expression[5]), as well as disorganized schizotypy

dimension (referring to disorganized thinking and behavior[5]). Some inventories also include additional dimensions, such as measures of impulsive/antisocial behavior.[6,7] This dimensional structure closely resembles the distinction of positive, negative, and disorganized symptoms in psychosis or schizophrenia.[8]

While schizotypal traits do not necessarily lead to schizophrenia, they are seen as an indicator of psychosis proneness, especially in dimensional models of psychopathology[2,9,10] and thus a marker of psychosis risk in the general population.[4]

Linking schizotypy as a dimensional marker of psychopathology to the neurobiology of the psychosis spectrum has resulted in several recent association studies with brain structure and function. A large ENIGMA study of brain volumes in healthy subjects has indicated correlations of schizotypy with regional volumes and overlaps with schizophrenia case–control studies.[11] Similarly, several smaller functional imaging studies have indicated similarities between schizotypy across healthy cohorts and changes seen in clinical schizophrenia.[12] In contrast, studies of the structural connectome and schizotypy are sparse.

Since schizophrenia has been conceptualized as a disorder of brain dysconnectivity[13] there is an increasing need to understand the relation of structural connectivity markers across the spectrum. This can be assessed with diffusion tensor imaging (DTI), which provides indicators of fiber integrity and orientation, in particular fractional anisotropy (FA) as well as axial diffusivity (AD) and radial diffusivity (RD).[14] Several studies, including larger multicenter designs, have mapped group-level differences between schizophrenia and healthy controls. A large ENIGMA study showed lower FA in the whole brain of schizophrenia patients with the largest effect in frontothalamic bundles,[15] while Vitolo et al.[16] also found numerous alterations, particularly in frontal, temporal and limbic regions. Recent findings implicate that especially the prefrontal cortex is less connected to other cortical regions.[17] Lener et al.[18] compared white-matter abnormalities in schizophrenia and SPD and found attenuated dysconnectivity in frontotemporal networks compared to healthy controls. Further studies from Hazlett et al.,[19] Sun et al.,[20] and Nakamura et al.[21] support these findings in schizotypal personality disorder (SPD).

In contrast, only a few studies examined DTI in schizotypy. Nelson et al.[22] found structural impairment in frontotemporal tracts using FA for the cognitive-perceptual (ie, positive) domain of SPQ. Further studies used a categorial approach, comparing individuals scoring high vs. low in total schizotypy. DeRosse et al.[23] found reduced FA in the frontal and temporal lobe, while Wang et al.[24] found higher connectivity probability between the right insula and the right frontal gyrus as well as the left precuneus and angular gyrus. Pfarr and Nenadić[25] also reported altered structural connectivity in thalamostriatal tracts with a fully dimensional approach using the recently developed Multidimensional Schizotypy Scale.[26] A most recent study[27] used graph-theory-based metrics on DTI and also implicated prefrontal nodes in schizotypy-related connectivity. These mentioned studies have been conducted in smaller samples and thus might lack statistical power to detect more minute associations in correlational designs. In addition, the nature of simple association designs limits the interpretation of findings. For example, it is unclear whether the effects of schizotypy on particular schizophrenia-associated fiber tracts might be related to genetic susceptibility to psychosis.

In the present study, we analyzed a larger sample (the sample size of previous studies ranged between 104, 138, 209, and 255[23–25,27]) to test for associations between the proposed schizotypy dimensions, using the 4-dimensional O-LIFE inventory, as well as for moderating effects of the polygenic risk for schizophrenia. To limit the number of statistical tests and thereby minimize multiple comparisons, we preselected 3 white-matter tracts. Those were identified in previous schizophrenia or schizophrenia spectrum case–control studies[28]; in particular, this included structural connectivity of prefrontal cortex and thalamo-frontal-striatal systems, esp. the anterior thalamic radiation (ATR) (connecting mediodorsal and anterior thalamus with prefrontal cortices), uncinate fascicle (UF) (connecting prefrontal and anterior/medial temporal lobes), and cingulum bundle (connecting prefrontal to posterior areas, including hippocampus). While our main hypothesis applied FA as a structural connectivity marker, we additionally examined the DTI parameters AD and RD. We expected differential effects across the 4 O-LIFE subscales (Unusual Experiences/positive schizotypy, Introvertive Anhedonia/negative schizotypy), (Cognitive Disorganization/disorganized schizotypy, and Impulsive Nonconformity/impulsive behavior), given that the previous DTI studies in schizophrenia also found different associations of symptom profiles with FA. To our knowledge, the current DTI studies on SZT do not provide a link to potential shared genetical underpinnings of the psychosis spectrum, for example, it is unclear whether associations between psychometric schizotypy and DTI parameters might be related to individual variation in genetic burden to schizophrenia. Given the availability of GWAS-based polygenic risk scores (PRS), individual SNP-based genetic liability can be assessed and included in statistical modeling of brain-schizotypy associations. For moderation analyses, we considered both PRS derived from the most recent schizophrenia GWAS,[29] as well as a novel polygenic score for resilience to schizophrenia.[30]

Methods

Study Participants

The study sample consisted of 346 psychiatrically healthy participants which had been recruited by email and public

Table 1. Descriptive Statistics of Age and O-LIFE, Including Cronbach's Alpha (n = 346)

Descriptives	Min	Max	Mean	Std. Deviation
O-LIFE UnEx	0	14	1.82	2.36
O-LIFE CogDis	0	21	5.25	4.30
O-LIFE IntAn	0	19	4.10	3.52
O-LIFE ImpNon	0	15	6.13	2.85
O-LIFE sum	3	54	17.30	8.59
Age	18	39	23.89	3.74
Sex		Frequency		Percent
Female		228		65.9
Male		118		34.1

advertisements as part of an ongoing study. All participants gave written informed consent to the procedure and were financially compensated afterwards. The local ethics committee (Ethics Committee of the School of Medicine, Philipps-University Marburg; protocol numbers 61/18 and 79/18) approved the study protocol according to the latest version of the Declaration of Helsinki (World Medical Association, 2013). We included native German-speaking Central European participants aged 18-40 years.

Exclusion criteria were current or history of psychiatric disorders or psychotherapeutic treatment, central nervous system neurological disorders, general intellectual impairment, learning disability (defined as IQ lower 80), substance abuse or dependence, traumatic brain injury or a BMI < 18 or > 35 and contraindications to MRI scanning, eg, uncontrolled physical disorders possibly interfering with scanning. The absence of a psychiatric history was ascertained using the SCID I screening questionnaire (Structured Clinical Interview for DSM-IV Axis I Disorders; SKID-I[31,32]) by trained raters, while IQ was estimated using the German MWT-B test, a vocabulary test similar to the British National Adult Reading Test (Multiple-Choice Vocabulary Intelligence Test B[33]).

Schizotypy Assessment/Phenotyping

For the assessment of schizotypal traits, we used the Oxford-Liverpool Inventory of Feelings and Experiences.[6,34] Each subject received a personalized link and completed the inventory online within 1 week of their MRI examination.[35]

The O-LIFE is based on a fully dimensional model of schizotypy. It assesses personality features of schizotypy and other traits like impulsiveness. Mason and Claridge used an explorational factor analysis based on multiple previous questionnaires like the Claridge-Schizotypy questionnaire and the Eysenck personality questionnaire.[36]

The O-LIFE contains 104 Items, which are divided into 4 domains: Unusual Experiences (UnEx), Cognitive Disorganization (CogDis), Introvertive Anhedonia (IntAn), and Impulsive Nonconformity (ImpNon). The Unusual Experiences subscale is related to positive facets of schizotypy, like magical thinking, assessed by items like "Do you believe in telepathy."[34] The Cognitive Disorganization subscale assesses cognitive impairment by using items like "Are you easily distracted when you read or talk to someone?."[34] While the Introvertive Anhedonia subscale reflects aspects of negative schizotypy referring to social withdrawal ("Do you feel that making new friends isn't worth the energy it takes?"[34]), Impulsive Nonconformity refers to impulsive antisocial aspects of negative schizotypy ("Do people who drive carefully annoy you?").[34]

Descriptives can be found in table 1. Cronbach's alpha was estimated for all subscales (UnEx: 0.73, CogDis: 0.83, IntAn: 0.77, ImpNon: 0.59); previous validation indicated Cronbach's alpha of 0.89 (UnEx), 0.87 (CogDis), 0.82 (IntAn) and 0.77 (ImpNon).[6]

DNA Analysis, Genotyping and Imputation

Blood samples were collected from all participants, and DNA was successfully extracted for 343 participants. The Infinium Global Screening Array-24 BeadChip (GSA, customized to include additional markers relevant to psychiatric disorders; Illumina, San Diego, CA, USA) was used for genome-wide genotyping. We applied the PLINK[37] software package to implement standard quality control procedures (e.g., sample call rate > 0.98; variant call rate > 0.98; Minor Allele Frequency > 0.01; removal of variants deviating from Hardy–Weinberg equilibrium with P < 1e-06; checking for sex mismatches and heterozygosity outlier). With the Haplotype Reference Consortium panel (rv1.1; www.haplotype-reference-consortium.org), the data was then imputed via Positional Burrows–Wheeler Transform. Variants with low prediction accuracy (info score < 0.6) were excluded from PRS calculation.

Polygenic Risk Score Calculation and Outlier Detection

We used summary statistics from the respective genome-wide association studies as provided by the Psychiatric

Genomics Consortium[29] and Hess[30] et al., and as detailed elsewhere[38] calculated PRS as the sum of the risk alleles (common variants with Minor Allele Frequency > 1%) weighed by their effect estimates. Based on the GWAS findings, we used the genome-wide significant threshold for the schizophrenia PRS ($P = 5e^{-8}$). As there were no genome-wide significant variants identified for schizophrenia resilience PRS, we chose the threshold reflecting the most significant association with resilience status in a case vs. control design ($P = .3$) in the original study.

Two pairs of cryptic relatives with pi-hat ≥ 0.125 were identified in the initial sample of 343 participants. One person was randomly excluded of each pair. We used PLINK v1.90b6.24 to control for genetic heterogeneity due to population structure and computed the first 8 multidimensional scaling (MDS) components based on pairwise identity-by-state distance matrix. They were included as covariates in all analyses. Additionally, 2 subjects were excluded because they were identified as genetic outliers with a distance from the mean of > 6 SD in the ancestry components. A final sample of 339 participants for moderation analyses remained.

MRI Data Acquisition

We used a 3 Tesla MRI Scanner with a standard 12-channel head matric Rx-coil (Siemens Magnetom, TrioTim syngo, Erlangen, Germany) to acquire T1-weighted and diffusion-weighted images as part of a larger scanning protocol. First T1-weighted images were acquired (TR 1900 ms; TE 2.26 ms; time of inversion 90 ms bandwidth 200 Hz/Px. 176 slices; slice thickness 1 mm; voxel resolution 1 mm × 1 mm × 1 mm; FOV 256 mm). Applying an EPI 2SD sequence and diffusion-mode MDDW (TR 7300 ms, TE 90 ms, 56 slices with 3 mm slice thickness, isotropic voxel resolution of 2.5 mm^3 × 2.5 mm^3 × 2.5 mm^3, FOV 256 mm), we obtained 2 × 30 diffusion-weighted and 4 nondiffusion-weighted images (b = 1000a/ mm^2) for each subject.

All images were visually inspected for structural pathologies before inclusion into the sample. As all subjects passed the quality assurance, the sample size remained at n = 346.

DTI Preprocessing

We used FSL software (version 6.0[39]) with the implemented Tract-Based Spatial Statistics.[40] The preprocessing pipeline included motion correction and Eddy-current-artifact-correction,[41] nonbrain tissue removal by visually selecting the fractional intensity threshold to generate a brain mask. Based on our anatomical hypothesis, we selected 3 tracts: ATR, cingulum bundle ("cingulum-cingulate gyrus" representing the anterior and "cingulum-hippocampus" representing the posterior part) and UF. For each of these tracts, we primarily computed FA for each subject. Additionally, AD and RD were computed for additional exploratory analyses. These images were nonlinear registered into the standard Montreal Neurological Institute space (MNI-152).[42] By calculating the average of these images, we generated a mean image for FA, AD and RD.

Thereupon a mean skeleton for FA, AD, and RD was created on which the mean image was projected with a threshold < 0.2 to exclude voxels lying in the gray matter or CSF.

We primarily examined FA, a commonly used marker for "integrity" of fiber tracts, which might be related to larger axon diameter or lower packing density facilitating diffusion in a tract.[43] In a second step we also tested the effects on "AD," indicating diffusion along the direction of the tract and "RD," indicating diffusion in orthogonal direction to the tract. These parameters are also influenced by both myelination and axon density.[43]

Statistical Analyses

We performed multiple regression analysis using the GLM module in FSL[39] (version 6.0), creating and estimating a separate model for each scale of the O-LIFE as well as the sum score considering age, sex, and total intracranial volume as covariates. For our main analysis of FA, we ran separate GLMs for the 4 schizotypy dimensions reflected in the O-LIFE. These 4 separate GLMs were repeated for RD and AD, respectively. To allow comparability with previous studies, we also ran additional GLM for O-LIFE total score, again, separately for FA, RD, and AD. All GLMs were performed within each of the selected tracts to limit search space and reduce potential false positives. The FSL-randomize tool was used to run nonparametric permutation analyses with 5000 permutations based on the Threshold-Free-Cluster-Enhancement option.[40]

Due to our hypotheses, analyses were restricted to bilateral masks of the FSL-defined ATR, Cingulum-Cingular Gyrus (anterior cingulum) Cingulum-Hippocampus (posterior cingulum bundle) and UF. Additionally, we controlled all p-values for multiple comparisons on the cluster-level using family-wise error rates (FWE), a standard procedure implemented in FSL.[39,44]

We labeled the significant clusters anatomically according to the JHU white-matter-tractography atlas[45] and considered all clusters larger than 10 voxels with FWE corrected p-values < 0.05 as significant.

Moderation and Mediation Analyses

We extracted mean FA values from the significant clusters from FSL. These cluster values were used as outcome variables in general linear regression models, tested with the GAMLj module[46] in jamovi[47] (version 2.4.11). We included the previously calculated MDS components,

Table 2. Statistical Results of the General Linear Model: O-LIFE Dimension as Predictors and Age and Sex as Covariates ($P < .05$ FWE Peak Level) Anatomical Labeling With JHU White-Matter Tractography Atlas[45]

O-LIFE Scores and Direction of Effect	Tract/Localization	*k*	*P*	Coordinates of Maximum-Peak Voxel in MNI Space (X/Y/Z)	Anatomical Labeling. JHU White-Matter Tractography Atlas
Fractional anisotropy (FA)					
Sum Positive correlation	Left cingulum-cingulate gyrus	583	.009	101/153/88	Genu of corpus callosum 45% Forceps minor 8% Cingulum (cingulate gyrus) L
UnEx Positive correlation	Right cingulum-hippocampus	26	.033	67/89/64	Cingulum (hippocampus) R 28% Cingulum (hippocampus) R
IntAn Negative correlation	Right uncinate fasciculus	14	.047	67/151/89	Anterior corona radiata R 26% Inferior fronto-occipital fasciculus R 14% Uncinate fasciculus R
CogDis positive correlation	Left cingulum-cingulate gyrus	174	.026	101/151/89	Genu of corpus callosum 34% Forceps minor 3% Cingulum (cingulate gyrus) L
Radial diffusivity (RD)					
Sum Negative correlation	Left cingulum-cingulate gyrus	468	.012	102/157/85	Genu of corpus callosum 58% Forceps minor 8% Cingulum (cingulate gyrus) L
UnEx Negative correlation	Left cingulum-hippocampus	124	.007	113/107/46	Cingulum (hippocampus) L 29% Cingulum (hippocampus) L
	Right cingulum-hippocampus	12	.042	68/90/64	Cingulum (hippocampus) R 38% Cingulum (hippocampus) R
IntAn Positive correlation	Right anterior thalamic radiation	48	.026	85/105/70	37% Anterior thalamic radiation R
ImpNon Negative correlation	Left anterior thalamic radiation	108	.024	97/107/87	37% Anterior thalamic radiation L
	Right anterior thalamic radiation	91	.032	79/101/86	13% Anterior thalamic radiation R
Axial diffusivity (AD)					
Sum Negative correlation	Left anterior thalamic radiation	93	.033	114/155/77	Anterior corona radiata L 29% Inferior fronto-occipital fasciculus L 17% Uncinate fasciculus L 11% Anterior thalamic radiation L
	Right anterior thalamic radiation	99	.028	68/164/94	8% Inferior fronto-occipital fasciculus R 8% Forceps minor 8% Anterior thalamic radiation R
	Left cingulum-hippocampus	12	.033	117/102/48	23% Cingulum (hippocampus) L
	Left uncinate fasciculus	130	.034	114/155/78	Anterior corona radiata L 34% Inferior fronto-occipital fasciculus L 22% Uncinate fasciculus L 21% Anterior thalamic radiation L
	Right uncinate fasciculus	52	.043	64/156/73	Anterior corona radiata R 18% Inferior fronto-occipital fasciculus R 3% Uncinate fasciculus R
	Right uncinate fasciculus	37	.045	58/137/66	External capsule R 32% Inferior fronto-occipital fasciculus R 17% Uncinate fasciculus R
UnEx Negative correlation	Left cingulum-hippocampus	73	.012	114/103/48	Cingulum (hippocampus) L 40% Cingulum (hippocampus) L
IntAn Negative correlation	Right anterior thalamic radiation	51	.015	85/111/70	45% Anterior thalamic radiation R

Table 2. Continued

O-LIFE Scores and Direction of Effect	Tract/Localization	*k*	*P*	Coordinates of Maximum-Peak Voxel in MNI Space (X/Y/Z)	Anatomical Labeling. JHU White-Matter Tractography Atlas
ImpNon Negative correlation	Left anterior thalamic radiation	92	.024	101/157/87	37% Anterior thalamic radiation L
	Right anterior thalami radiation	197	.009	97/157/87	8% Inferior fronto-occipital fasciculus R 8% Anterior thalamic radiation R
CogDis Negative correlation	Left anterior thalamic radiation	379	.01	114/155/78	Anterior corona radiata L 34% Inferior fronto-occipital fasciculus L. 22% Uncinate fasciculus L. 21% Anterior thalamic radiation L
	Left anterior thalamic radiation	35	.033	109/174/84	58% Forceps minor 11% Anterior thalamic radiation L 3% Uncinate fasciculus L 3% Inferior fronto-occipital fasciculus L
	Left anterior thalamic radiation	13	.046	106/178/66	58% Forceps minor 11% Uncinate fasciculus L 8% Inferior fronto-occipital fasciculus L 8% Anterior thalamic radiation L
	Left anterior thalamic radiation	10	.046	102/182/66	50% Forceps minor 8% Uncinate fasciculus L 3% Inferior fronto-occipital fasciculus L 3% Anterior thalamic radiation L
	Left uncinate fasciculus	489	.007	114/155/78	Anterior corona radiata L 34% Inferior fronto-occipital fasciculus L 22% Uncinate fasciculus L 21% Anterior thalamic radiation L
	Left uncinate fasciculus	106	.022	116/144/80	Anterior corona radiata L 24% Inferior fronto-occipital fasciculus L 8% Uncinate fasciculus L 5% Superior longitudinal fasciculus L
	Right uncinate fasciculus	166	.012	61/140/77	External capsule R 26% Inferior fronto-occipital fasciculus R, 3% Uncinate fasciculus R

Average/peak voxel Cohen's *d* for FA results were: Sum: 0.109/0.177, UnEx: 0.167/0.192, IntAn: 0.170/0.183, CogDis: 0.131/0.184.
k = number of voxels.

O-LIFE dimension, age, sex, TIV, and PRS as covariates, and the interaction variable of the O-LIFE dimension and PRS as predictor.

Results

Association of DTI Parameters With O-LIFE Sum Score

The O-LIFE sum score showed (a) a positive correlation with FA ($P = .009$; FWE cluster-level) in the left anterior cingulum bundle, (b) a negative correlation with AD in the left and right ATR (left: $P = .033$; right $P = .028$; FWE cluster-level), left posterior cingulum bundle ($P = .033$; FWE cluster-level) and left and right UF (left: $P = .034$; right: $P = .028$ and $P = .045$; FWE cluster-level, and (c) a negative correlation with RD in the left anterior cingulum ($P = .012$; FWE cluster-level). An overview of the statistical results can be found in table 2, see Figure 1 for a graphic depiction.

Association of DTI Parameters With O-LIFE Subscores/Schizotypy Dimensions

The Cognitive Disorganization dimension was (a) positively correlated with FA in the left anterior cingulum ($p = .026$; FWE cluster-level) and (b) negatively correlated with AD in 4 clusters in the left ATR ($p1 = 0.001$, $p2 = 0.033$, $p3 = 0.046$, $p4 = 0.046$; FWE cluster-level), as

Table 3. Moderation Analyses With General Linear Model: Considering MDS Components, O-LIFE Dimension, Age, Sex, TIV, and PRS as Covariates, and the Interaction Variable of the O-LIFE Dimension and PRS as Predictor

Interaction Term	Significant Cluster From Previous Analysis	Estimate	95% CI (Lower Limit/Upper Limit)	*P*-Value of Estimate
Polygenic risk score for schizophrenia				
Unusual experiences	Right cingulum-hippocampus	0.0958	−0.109/0.301	.359
Introvertive anhedonia	Right uncinate fasciculus	0.0366	−0.181/0.108	.619
Cognitive disorganization	Left cingulum-cingulate gyrus	0.162	0.0102/0.315	.037
Sum score	Left cingulum-cingulate gyrus	0.0138	−0.0505/0.0782	.673
Polygenic resilience score for schizophrenia				
Unusual experiences	Right cingulum-hippocampus	0.974	−0.766/2.715	.272
Introvertive anhedonia	Right uncinate fasciculus	0.159	−1.88/1.56	.856
Cognitive disorganization	Left cingulum-cingulate gyrus	0.216	−1.33/1.77	.784
Sum score	Left cingulum-cingulate gyrus	−0.222	−0.805/0.361	.454

well as the left and right UF (left: $P = .007$ and $P = .033$; right $P = .012$; FWE cluster-level).

The Unusual Experiences dimension showed (a) a positive association with FA the right posterior Cingulum ($P = .033$; FWE cluster-level), a negative association with (b) AD in the left posterior cingulum ($P = .012$; FWE cluster-level and c) RD in the left and right posterior cingulum (left: $P = .007$; right: $P = .042$; FWE cluster-level).

Significant results regarding the introvertive anhedonia dimension were (a) a negative correlation with FA in the right UF ($p = .047$; FWE cluster-level), (b) a negative correlation with AD ($P = .015$; FWE cluster-level), and (c) RD ($P = .026$; FWE cluster-level) in the right ATR.

No significant correlations were found for the impulsive nonconformity scale with (a) FA, but negative correlations in the ATR on both sides with (b) AD (left. $P = .024$; right: $P = .009$; FWE cluster-level, and (c) RD (left $P = .024$; right: $P = .032$; FWE cluster-level).

Interaction Between Schizotypy and Schizophrenia Polygenic Risk Score

We found a significant interaction between disorganized schizotypy and PRS in the above-reported cluster in the anterior cingulum bundle ($P = .037$). Negative, positive, or overall schizotypy did not show significant interactions with PRS. We did not find significant interactions between any of the O-LIFE scores and the PRS for resilience to schizophrenia. Results can be found in Figure 2 and table 3.

Discussion

In this study, we hypothesized an association between the structural connectivity and psychometric schizotypy in the ATR, the UF and the cingulum bundle—3 of the fiber tracts most commonly associated with schizophrenia spectrum pathology. While all these tracts provide connectivity of prefrontal areas to other brain areas, the ATR is crucial for the fronto-thalamo-striatal system, and the UF connects the PFC with the anterior temporal lobe and the cingulum bundle proceeds toward the parietal and temporal areas particularly including the hippocampus. In line with our hypothesis of differential effects, our findings demonstrate that the 3 schizotypy dimensions map differently onto these tract systems: Negative schizotypy was negatively correlated with FA in the UF/fronto-thalamo-striatal system, while positive and disorganized schizotypy mapped onto anterior and posterior cingular FA respectively. Interestingly, associations of the schizotypy sum score appeared to be driven by the disorganized dimension, as the findings in those 2 parameters mostly overlap. This finding illustrates that even in the nonclinical part of the wider psychosis spectrum, different aspects of the psychosis risk phenotype link to particular anatomical substrates. Studies focusing on overall or sum scores of schizotypy are likely to be either actually driven by one particular aspect (such as disorganized schizotypy as in our study) or fail to establish an association based on the relatively smaller effects of each facet as they contribute to the sum scores.

As our study overcomes several limitations of some of the (few) previous studies, our findings also provide novel insights when contrasted against previous findings based on diverging approaches. First, we did not confirm previous findings in schizotypy sum sores. DeRosse et al.,[23] Wang et al.[24] and Messaritaki et al.[27] compared high vs. low schizotypy based on total scores, thus excluding the possibility of analyzing the impact of different schizotypy dimensions and restricting the comparison to dichotomized extreme groups. Wang et al.[24] and Messaritaki et al.[27] used network-based approaches. Thus, their findings of higher structural connectivity using probabilistic tractography[24] and graph theoretical measures[27] cannot be directly compared to our TBSS analyses. Rather, their findings indicate that network properties of FA variation might link to schizotypy in addition to direct correlations with singular ROIs. DeRosse et al.[23] found higher asymmetry in the UF, which equally to our finding of lower FA in negative schizotypy can be seen as further evidence for lateralization effects in schizotypy. We cannot compare

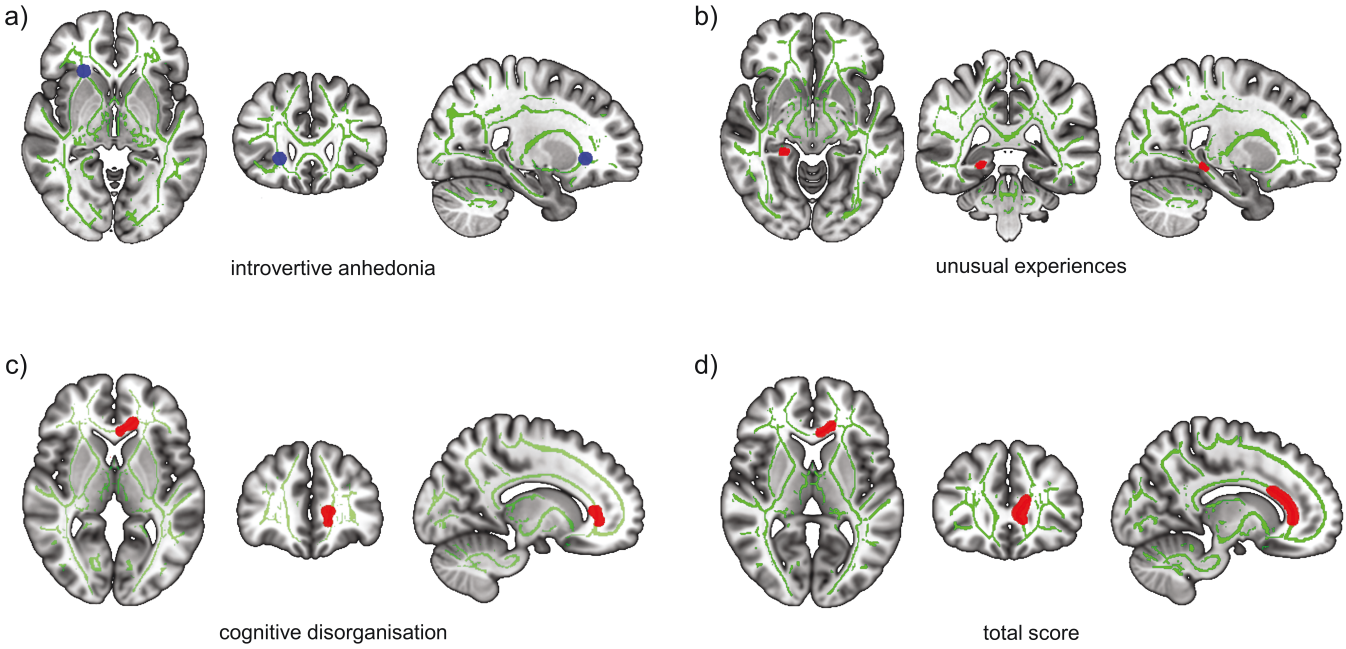

Fig. 1. Associations between O-LIFE and FA, FWE peak level corrected. (A) Negative association between O-LIFE introvertive anhedonia and FA in right UF, (B) positive association between O-LIFE unusual experiences and FA posterior cingulum bundle, (C) positive association between O-LIFE cognitive disorganization and FA in anterior cingulum bundle. illustrations were prepared using MRIcron (Version 1.2.20220720, https://www.nitrc.org/projects/mricron). The peak voxel was used for cutting plane coordinates.

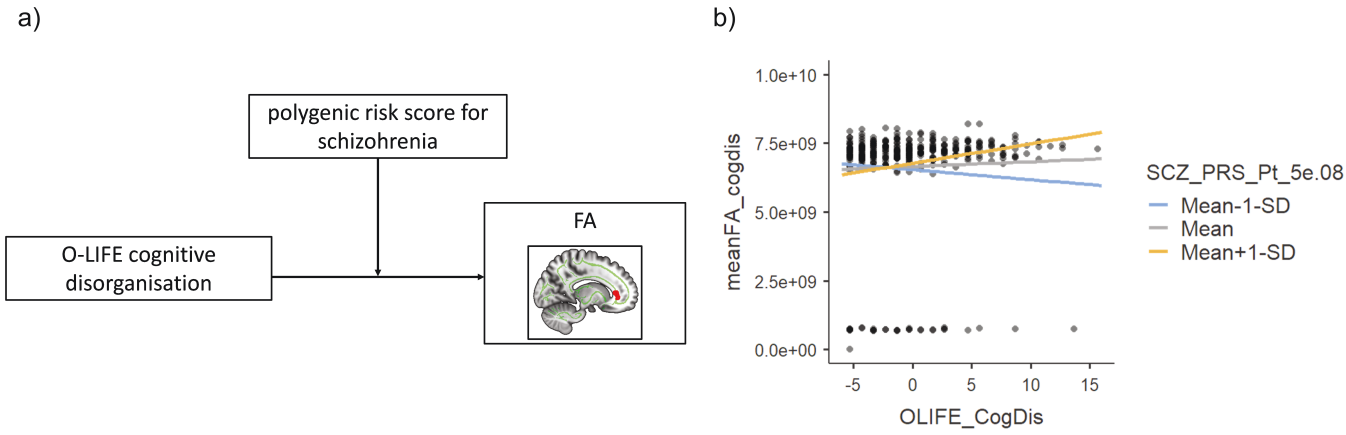

Fig. 2. (A) visualization of the conceptual moderation model and (B) simple effects plot of moderation effect for O-LIFE cognitive disorganization.

their finding of lower FA in the inferior fronto-occipital fasciculus (IFOF) to our findings as the IFOF was not included in our hypothesis.

Second, 2 previous studies using correlational approaches across the schizotypy dimensions[22,25] also showed only limited overlap with our findings. The negative correlation between negative schizotypy and FA in the right UF was not identified in these studies, while their findings in positive and disorganized schizotypy stand in contrast to ours.

Positive schizotypy showed a negative association of FA in frontotemporal and fronto-occipital regions in contrast to our findings of a positive association of FA in anterior cingular regions.[22] Similarly, disorganized schizotypy has previously been associated with lower FA in fronto-thalamic and fronto-occipital tracts,[25] but with higher FA in the posterior cingulum in our study.

Even though we might consider discrepancies between samples and used inventories as probable contributors to these differences, this does not sufficiently explain the opposed direction of effects since subscales between inventories are generally correlated.[36]

More importantly, our study is the first to establish a link between schizotypy, connectivity, and genetics, as we

identify only the correlation of FA to disorganized schizotypy to be moderated by schizophrenia polygenic risk.

Schizotypy scores in our sample were in the lower to medium range, as is to be expected for a healthy sample. This limits our ability to infer relations in high schizotypy or clinical samples. Additional studies, for example, using cohorts enriched for higher schizotypy scores or clinical cases, would be needed to draw robust inferences across the entire psychosis spectrum. Yet our study allows limited comparison to case–control studies of SPD, where we find some areas of overlap. Similar to our findings in negative schizotypy, SPD patients showed FA reductions in the right UF.[21] However, in SPD, additional regions were involved with lower FA in frontal, temporal and cingular white matter.[18,19,21] Higher FA, equivalent to our findings in positive, disorganized, and overall schizotypy, was described in the anterior cingulum in one study with SPD patients.[19]

Correlating FA with schizotypal personality traits in clinical SPD revealed significant associations with negative schizotypy (assessed with SPQ interpersonal factor) in the right UF[21] (equivalent to our finding) and additionally in the cingulum.[19] On the other hand, no correlation of positive, disorganized, or overall schizotypy with white-matter alterations was found in SPD. This could indicate possible neurobiological progress from healthy individuals to SPD in the negative schizotypy phenotype, with cingular regions becoming additionally involved.

Overall, structural connectivity seems to decrease across the psychosis spectrum from traits in healthy participants to patients with schizophrenia, whereas the number of affected areas seems to increase.[48] Findings of a large ENIGMA study show that the whole brain is affected with a focus on frontotemporal areas.[15,17] Our study found lower FA only in the UF associated with negative schizotypy. The UF seems to play a small role in schizophrenia[17] but is associated with negative symptoms.[49] While we found positive associations between FA and positive, disorganized, and overall schizotypy in the cingulum bundle, it is associated with lower FA and cognitive dysfunction in schizophrenia.[50] Previous analyses by Yang et al. correlations of FA with symptom severity revealed a pattern consistent with our findings: while positive symptom severity (positive schizotypy) was associated with higher FA, negative symptom severity (negative schizotypy) was associated with lower FA.[51]

If psychosis proneness progresses into clinical manifestations like SPD or schizophrenia, additional effects could be caused by the onset of a pathological process itself (eg, altered plasticity across neural networks), but also with effects treatment. Increased connectivity in healthy individuals with high schizotypal traits might then be understood as compensation within interconnected systems. Longitudinal studies would be needed to better understand the evolution of connectivity parameters. A recent study of adolescent individuals has shown that cortical thickness changes over a 5-year period are associated with schizotypy,[52] but to our knowledge, similar DTI findings are lacking.

Raine[53] hypothesized 2 subgroups of schizotypy (neurodevelopmental schizotypy vs "pseudoschizotypy"), where the disorganized traits are more common in the former group which also has a higher genetic risk for schizophrenia. While this model has not been widely adopted, it highlights the differential role of genetic schizophrenia risk on brain function and structure. In contrast, our lack of associations with the new polygenic score for schizophrenia resilience might be explained by this PRS targeting mechanisms that are related mostly to biological processes important to the transition from proneness to disease—they hence might be less tightly linked to proneness itself.

Limitations of our study include the lack of direct comparison with schizophrenia spectrum pathology (eg, SPD) or clinical high-risk cases as well as effects of other disease spectra. While our study was larger than previously published studies, replication in new samples as well as multicenter initiative (eg, ENIGMA) might be necessary to detect more minute effects as well as a whole brain approach, including additional fiber tracts.

In conclusion, our studies demonstrate the association of different facets of schizotypy to the ATR, UF, and cingulum—3 major tracts involved in the schizophrenia spectrum. More importantly, it is only for disorganized schizotypy that we demonstrate a moderating effect of polygenic schizophrenia risk to impact on these associations, showing that genetic factors (at least those relevant to developing schizophrenia) show differential impact on brain systems relevant to particular phenotype facets.

Author Contribution

J.H.: Data curation, Formal analysis, Methodology, Software, Visualization, Writing – original draft. T.M.: Data curation, Methodology, Project administration, Supervision, Validation, Writing – review & editing. C.M.: Methodology, Resources, Software, Writing – review & editing. P.H.: Methodology, Resources, Software, Writing – review & editing. A.J.F.: Methodology, Resources, Software, Writing – review & editing. M.M.N.: Methodology, Resources, Software, Writing – review & editing. I.N.: Funding acquisition, Methodology, Project administration, Resources, Software, Supervision, Validation, Writing – original draft.

Funding

This study was supported by a research grant of the University Medical Center Giessen and Marburg (UKGM) grants to I.N. (11/2017 MR and 05/2018 MR). This work was partially supported through Forschungscampus Mittelhessen (FCMH) FlexiFunds grants (2017_2_1_5 and 2018_2_1_1 to I.N.). I.N. is a PI of and supported by the DYNAMIC center, which is

funded by the LOEWE program of the Hessian Ministry of Science and Arts (Grant Number: LOEWE1/16/519/03/09.001(0009)/98).

Conflicts of Interest

The authors have declared that there are no conflicts of interest in relation to the subject of this study.

References

1. Ettinger U, Meyhöfer I, Steffens M, Wagner M, Koutsouleris N. Genetics, cognition, and neurobiology of schizotypal personality: a review of the overlap with schizophrenia. *Front Psychiatry.* 2014;5:18.
2. Nelson MT, Seal ML, Pantelis C, Phillips LJ. Evidence of a dimensional relationship between schizotypy and schizophrenia: a systematic review. *Neurosci Biobehav Rev.* 2013;37:317–327.
3. Barrantes-Vidal N, Grant P, Kwapil TR. The role of schizotypy in the study of the etiology of schizophrenia spectrum disorders. *Schizophr Bull.* 2015;41:S408–S416.
4. Taylor JH, Calkins ME, Gur RE. Markers of psychosis risk in the general population. *Biol Psychiatry.* 2020;88:337–348.
5. Kwapil TR, Barrantes-Vidal N. Schizotypy: looking back and moving forward. *Schizophr Bull.* 2015;41:S366–S373.
6. Mason O, Claridge G, Jackson M. New scales for the assessment of schizotypy. *Pergamon*. 1995;18:7–13.
7. Chapman LJ, Chapman JP, Numbers JS, Edell WS, Carpenter BN, Beckfield D. Impulsive nonconformity as a trait contributing to the prediction of psychotic-like and schizotypal symptoms. *J Nerv Ment Dis.* 1984;172:681–691. https://pubmed.ncbi.nlm.nih.gov/6491653/
8. Polner B, Faiola E, Urquijo MF, et al. The network structure of schizotypy in the general population. *Eur Arch Psychiatry Clin Neurosci.* 2019;271:635–645.
9. Debbané M, Barrantes-Vidal N. Schizotypy from a developmental perspective. *Schizophr Bull.* 2015;41:S386–S395.
10. Debbané M, Eliez S, Badoud D, Conus P, Flückiger R, Schultze-Lutter F. Developing psychosis and its risk states through the lens of schizotypy. *Schizophr Bull.* 2015;41:S396–S407.
11. Kirschner M, Hodzic-Santor B, Antoniades M, et al. Cortical and subcortical neuroanatomical signatures of schizotypy in 3004 individuals assessed in a worldwide ENIGMA study. *Mol Psychiatry.* 2021;27:1167–1176. https://pubmed.ncbi.nlm.nih.gov/34707236/
12. Tonini E, Quidé Y, Kaur M, Whitford TJ, Green MJ. Structural and functional neural correlates of schizotypy: a systematic review. *Psychol Bull.* 2021;147:828–866.
13. Friston K, Brown HR, Siemerkus J, Stephan KE. The dysconnection hypothesis (2016). *Schizophr Res.* 2016;176:83–94.
14. Tournier J-D, Mori S, Leemans A. Diffusion tensor imaging and beyond. *Magn Reson Med.* 2011;65:1532–1556. https://pubmed.ncbi.nlm.nih.gov/21469191/
15. Kelly S, Jahanshad N, Zalesky A, et al. Widespread white matter microstructural differences in schizophrenia across 4322 individuals: results from the ENIGMA Schizophrenia DTI Working Group. *Mol Psychiatry.* 2017;23:1261–1269.
16. Vitolo E, Tatu MK, Pignolo C, et al. White matter and schizophrenia: a meta-analysis of voxel-based morphometry and diffusion tensor imaging studies. *Psychiatry Res Neuroimaging*. 2017;270:8–21.
17. Zhou Y, Fan L, Qiu C, Jiang T. Prefrontal cortex and the dysconnectivity hypothesis of schizophrenia. *Neurosci Bull.* 2015;31:207–219.
18. Lener MS, Wong E, Tang CY, et al. White matter abnormalities in schizophrenia and schizotypal personality disorder. *Schizophr Bull.* 2014;41:300–310.
19. Hazlett EA, Goldstein KE, Tajima-Pozo K, et al. Cingulate and temporal lobe fractional anisotropy in schizotypal personality disorder. *Neuroimage.* 2011;55:900–908.
20. Sun Y, Zhang L, Ancharaz SS, et al. Decreased fractional anisotropy values in two clusters of white matter in patients with schizotypal personality disorder: a DTI study. *Behav Brain Res.* 2016;310:68–75.
21. Nakamura M, McCarley RW, Kubicki M, et al. Fronto-temporal disconnectivity in schizotypal personality disorder: a diffusion tensor imaging study. *Biol Psychiatry.* 2005;58:468–478.
22. Nelson MT, Seal ML, Phillips LJ, Merritt AH, Wilson R, Pantelis C. An investigation of the relationship between cortical connectivity and schizotypy in the general population. *J Nerv Ment Dis.* 2011;199:348–353.
23. DeRosse P, Nitzburg GC, Ikuta T, Peters BD, Malhotra AK, Szeszko PR. Evidence from structural and diffusion tensor imaging for frontotemporal deficits in psychometric schizotypy. *Schizophr Bull.* 2015;41:104–114.
24. Wang Y-M, Cai X-L, Zhang R-T, et al. Altered brain structural and functional connectivity in schizotypy. *Psychol Med.* 2020;5:834–843.
25. Pfarr J-K, Nenadić I. A multimodal imaging study of brain structural correlates of schizotypy dimensions using the MSS. *Psychiatry Research. Neuroimaging*. 2020;302:111104.
26. Kwapil TR, Gross G, Silvia P, Raulin M, Barrantes N. *Multidimensional Schizotypy Scale Manual v2.9*; 2021.
27. Messaritaki E, Foley S, Barawi K, Ettinger U, Jones DK. Increased structural connectivity in high schizotypy. *Network Neuroscience (Cambridge, Mass.)*. 2023;7:213–233.
28. Siever LJ, Davis KL. The pathophysiology of schizophrenia disorders: perspectives from the spectrum. *Am J Psychiatry.* 2004;161:398–413. https://pubmed.ncbi.nlm.nih.gov/14992962/
29. Trubetskoy V, Pardiñas AF, Qi T, et al; Indonesia Schizophrenia Consortium. Mapping genomic loci implicates genes and synaptic biology in schizophrenia. *Nature.* 2022;604:502–508.
30. Hess JL, Tylee DS, Mattheisen M, et al; Schizophrenia Working Group of the Psychiatric Genomics Consortium. A polygenic resilience score moderates the genetic risk for schizophrenia. *Mol Psychiatry.* 2019;26:800–815.
31. Mori S, Wakana S, Nagae-Poetscher LM, van Zijl PCM. The structured clinical interview for DSM-IV axis I disorders (SCID-I) and the structured clinical interview for DSM-IV axis II disorders (SCID-II); 2004. https://psycnet.apa.org/record/2004-12821-011
32. Münster RD, Wittchen H-U, Zaudig M, Fydrich T. SKID Strukturiertes Klinisches Interview für DSM-IV. Achse I und II. Göttingen: Hogrefe, DM 158,-. Hiller, W., Zaudig, M. & Mombour, W. (1997). IDCL Internationale Diagnosen Checklisten für DSM-IV und ICD-10. Göttingen: Hogrefe, DM 198,- bzw. DM 239,-. *Zeitschrift für Klinische Psychologie und Psychotherapie*. 19971999;28:68–70.
33. Lehrl S, Triebig G, Fischer B. Multiple choice vocabulary test MWT as a valid and short test to estimate premorbid intelligence. *Acta Neurol Scand.* 1995;91:335–345.

34. Mason O, Claridge G. The Oxford-Liverpool Inventory of Feelings and Experiences (O-LIFE): further description and extended norms. *Schizophr Res.* 2006;82:203–211.
35. SoSci Survey ► professionelle Onlinebefragung made in Germany. Updated September 26, 2023. Accessed September 26, 2023. https://www.soscisurvey.de/
36. Pfarr J-K, Meller T, Evermann U, Sahakyan L, Kwapil TR, Nenadić I. Trait schizotypy and the psychosis prodrome: current standard assessment of extended psychosis spectrum phenotypes. *Schizophr Res.* 2023;254:208–217.
37. Purcell S, Neale B, Todd-Brown K, et al. PLINK: a tool set for whole-genome association and population-based linkage analyses. *Am J Hum Genet.* 2007;81:559–575.
38. Koutsouleris N, Dwyer DB, Degenhardt F, et al; PRONIA Consortium. Multimodal machine learning workflows for prediction of psychosis in patients with clinical high-risk syndromes and recent-onset depression. *JAMA Psychiatry*. 2021;78:195–209.
39. Jenkinson M, Beckmann CF, Behrens TEJ, Woolrich MW, Smith SM. FSL. *Neuroimage.* 2011;62:782–790.
40. Smith SM, Jenkinson M, Johansen-Berg H, et al. Tract-based spatial statistics: voxelwise analysis of multi-subject diffusion data. *Neuroimage*. 2006;31:1487–1505.
41. Andersson JLR, Sotiropoulos SN. An integrated approach to correction for off-resonance effects and subject movement in diffusion MR imaging. *Neuroimage.* 2015;125:1063–1078.
42. Fonov VS, Evans AC, McKinstry RC, Almli CR, Collins DL. Unbiased nonlinear average age-appropriate brain templates from birth to adulthood. *Neuroimage.* 2009;47:S102. https://www.sciencedirect.com/science/article/pii/S1053811909708845
43. Alexander AL, Lee JE, Lazar M, Field AS. Diffusion tensor imaging of the brain. *Neurotherapeutics*. 2007;4:316–329. https://pubmed.ncbi.nlm.nih.gov/17599699/
44. Winkler AM, Ridgway GR, Webster MA, Smith SM, Nichols TE. Permutation inference for the general linear model. *Neuroimage.* 2014;92:381–397.
45. Mori S, Wakana S, Nagae-Poetscher LM, van Zijl P. MRI atlas of human white matter. *AJNR Am J Neuroradiol.* 2006;27:1384–1385.
46. GAMLj. General analyses for the linear model in Jamovi. Updated November 8, 2023. Accessed January 9, 2024. https://gamlj.github.io/
47. Jamovi. Open statistical software for the desktop and cloud. Updated December 21, 2023. Accessed January 9, 2024. https://www.jamovi.org/
48. Attademo L, Bernardini F, Verdolini N. Neural correlates of schizotypal personality disorder: a systematic review of neuroimaging and EEG Studies. *Curr Med Imaging*. 2021;17:1283–1298.
49. Voineskos AN, Foussias G, Lerch J, et al. Neuroimaging evidence for the deficit subtype of schizophrenia. *JAMA Psychiatry*. 2013;70:472–480.
50. Kubicki M, Westin C-F, Nestor PG, et al. Cingulate fasciculus integrity disruption in schizophrenia: a magnetic resonance diffusion tensor imaging study. *Biol Psychiatry.* 2003;54:1171–1180.
51. Yang X, Cao D, Liang X, Zhao J. Schizophrenia symptomatic associations with diffusion tensor imaging measured fractional anisotropy of brain: a meta-analysis. *Neuroradiology.* 2017;59:699–708.
52. Derome M, Tonini E, Zöller D, Schaer M, Eliez S, Debbané M. Developmental trajectories of cortical thickness in relation to schizotypy during adolescence. *Schizophr Bull.* 2020;46:1306–1316.
53. Raine A. Schizotypal personality: neurodevelopmental and psychosocial trajectories. *Annu Rev Clin Psychol.* 2006;2:291–326.